

Supplementary Information

**Solid acid catalysed esterification of dicyclopentadiene with organic acids
to bio-based functional monomers†**

Sang-Ho Chung,^{a‡} Marilena Demetriou,^a Hongqi Wang,^a N. Raveendran Shiju^{*a}

^a Van 't Hoff Institute for Molecular Sciences, University of Amsterdam, P.O. Box 94157, 1090 GD Amsterdam, The Netherlands.

[‡] *Current address: KAUST Catalysis Center (KCC), King Abdullah University of Science and Technology, Thuwal 23955, Saudi Arabia.*

* E-mail: (N.R.S.) n.r.shiju@uva.nl

Methods

Materials. DCPD (95%, stabilized) and LA (98%) were purchased from Alfa Aesar GmbH & Co KG. Formic acid (98%), acetic acid (99%) and butyric acid (99%) were obtained from Fluka, Sigma Aldrich Chemie B.V., and VWR International B.V., respectively. 1,4-dioxane (99.8%) and toluene (98%, ACS, Reag. Ph. Eur.) were obtained from Biosolve B.V. and VWR International B.V., respectively. Hexanoic acid (99%), magnesium sulfate anhydrous ($\geq 99.5\%$), Amberlyst 15 (hydrogen and wet form), Amberlyst 35 (wet form), Amberlyst 70 (wet) were purchased from Sigma Aldrich (Rohm and Haas). The chemicals and catalysts were used without further purification.

Esterification of DCPD with biomass-derived acids. For the esterification of DCPD with LA, the reaction was performed in the round bottom flask and the liquid samples were periodically collected at certain time intervals. Typically, DCPD (0.5 mL, 3.7 mmol) and the equimolar carboxylic acids were magnetically stirred with the catalyst (0.5 g) in toluene (25 mL) at 80°C for 4 h. 1,4-dioxane was used as an internal standard (volume ratio of the solvent and the internal standard = 100:1). The tracing water in the reaction samples was removed adding the excess amount of anhydrous magnesium sulfate. The esterification of DCPD with other organic acids were performed using parallel autoclaves (Parr) with Teflon liners. The reactant conversions and the product selectivity were analyzed by GC-FID (PerkinElmer Clarus 580 GC) with the HP-5 column using He as the carrier gas. For the purification of the reaction products, the solvent was evaporated first from the reaction mixture using rotary evaporator under reduced pressure. The residue mixture was separated by column chromatography using silica gel as a stationary phase. The products were eluted with ethyl acetate/petroleum ether (volume ratio of 1:19) and the amount of ethyl acetate was increased gradually. After the evaporation of the solvent, the resulted esters were analyzed with ^1H NMR (Bruker, 400 MHz). Several samples were analyzed by GC-MS with filament ionizing voltage at 70 V and the related mass spectra were collected on the mass spectrometer (JEOL, AccuTOF LC, JMS-T100LP).

Structure of DCPD-LA

Detailed ^1H NMR assignments of DCPD-LA. ^1H NMR (400 MHz, Chloroform-d) δ 5.62 (ddq, $J = 6.2, 4.2, 2.1$ Hz, 1H), 5.37 (ddd, $J = 8.3, 5.8, 2.6$ Hz, 1H), 4.63 – 4.50 (m, 1H), 2.66 (t, $J = 6.5$ Hz, 2H), 2.58 – 2.42 (m, 4H), 2.12 (s, 3H), 2.04 (s, 1H), 2.03 – 1.90 (m, 2H), 1.93 – 1.77 (m, 1H), 1.78 – 1.63 (m, 1H), 1.34 (ddt, $J = 17.1, 13.9, 3.8$ Hz, 1H), 1.29 – 1.16 (m, 2H). (b) ^1H NMR spectrum of DCPD. DCPD: ^1H NMR (400 MHz, Chloroform-d) δ 5.93 – 5.81 (m, 4H), 5.41 (ddt, $J = 12.0, 7.6, 3.9$ Hz, 3H), 3.13 (ddq, $J = 8.4, 4.1, 1.9$ Hz,

2H), 2.79 (d, $J = 6.7$ Hz, 1H), 2.79 (s, 1H), 2.70 (s, 2H), 2.73 – 2.59 (m, 2H), 2.11 (ddt, $J = 17.3, 10.3, 2.1$ Hz, 2H), 1.54 (dt, $J = 16.8, 3.6, 1.9$ Hz, 2H), 1.40 (dd, $J = 8.0, 1.8$ Hz, 2H), 1.21 (s, 1H).

Fig. S1 is shown the GC-MS analysis result of the DCPD-LA. The fragmentation indicates that the product is related to DCPD (the molar mass of DCPD is 132 g mol^{-1}), to cyclopentene (fragment at 67 g mol^{-1}) and LA (fragment at 117 g mol^{-1}).

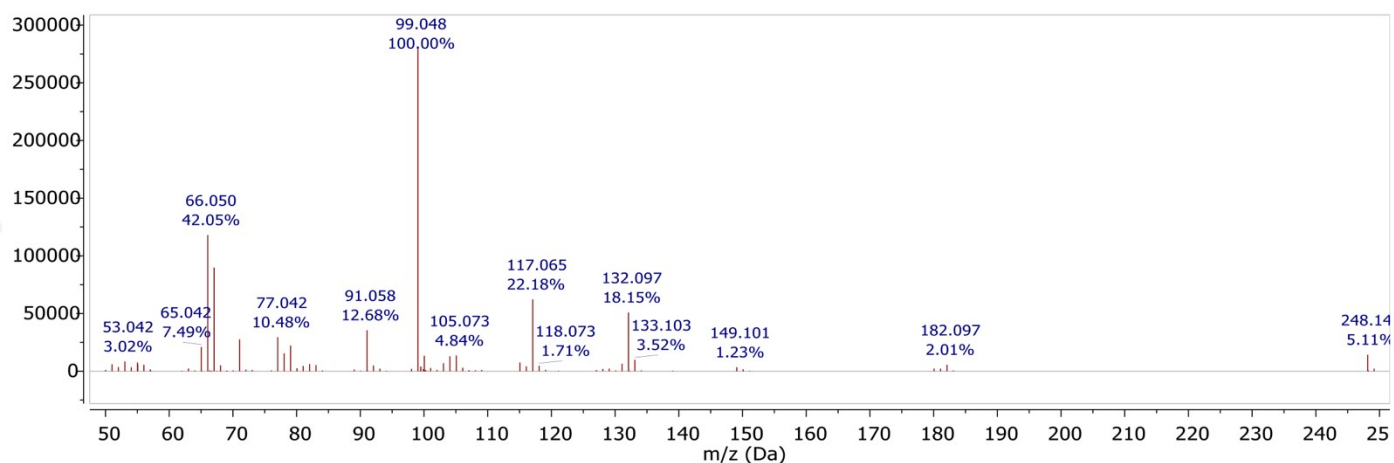


Fig. S1. GC-MS result and fragmentation of DCPD-LA.

^1H NMR spectra of two possible isomers of DCPD-LA ester were simulated using ChemDraw (PerkinElmer, version 20.1.1.125): one with the esterification in the norbornene ring (Fig. S2a) and the other in CPD ring (Fig. S2b). In case that the esterification takes place in the norbornene, two reduced peaks are expected in the region of 5.5-6.5 ppm (Fig. S2a), while in the case that the esterification does in the cyclopentene side, only one ^1H NMR peak in the region of ~ 6 ppm (Fig. S2b). Comparison between the simulated and the experimental ^1H NMR spectra, it can be elucidated that the double bond in the norbornene side reacted to form DCPD-LA ester during the esterification between DCPD and LA (Fig. 1b).

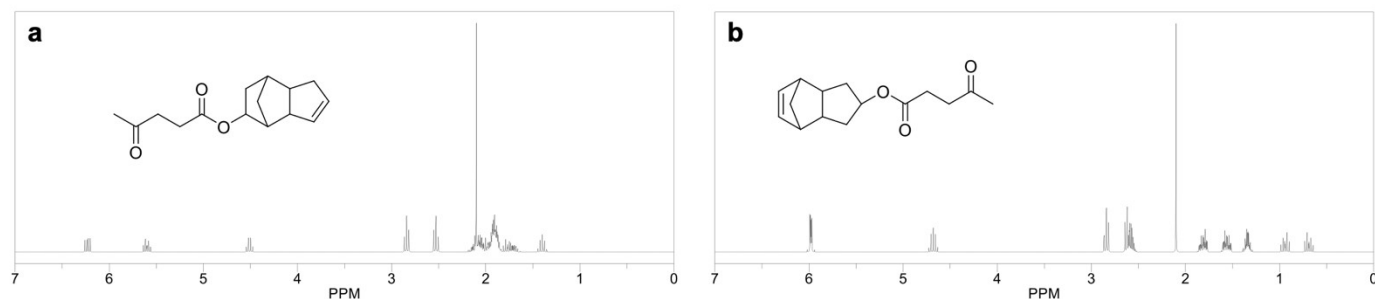


Fig. S2. Expected ^1H NMR spectra of DCPD-LA when the esterification occurs (a) on the norbornene ring and (b) on the cyclopentene ring.

Physicochemical properties of Amberlyst resin catalysts

Table S1. Properties of different types of Amberlyst catalysts.

Catalyst	Surface area (m ² g ⁻¹)	Average pore diameter (Å)	Maximum operating temperature (°C)	Concentration of acid sites (eq. kg ⁻¹)	Moisture content (%)
Amberlyst-15 (hydrogen form)	53	300	120	≥ 5.0	≤ 1.6
Amberlyst-15 (wet form)	53	300	120	≥ 4.95	52 – 57
Amberlyst-35 (wet form)	50	300	150	≥ 5.40	51 – 57
Amberlyst-70 (wet form)	36	220	190	≥ 2.55	52 – 57

Structure of DCPD-OH

Detailed ¹H NMR assignments of DCPD-OH. DCPD-OH: ¹H NMR (400 MHz, Chloroform-d) δ 5.61 (dq, J = 4.3, 2.0 Hz, 1H), 5.37 (tt, J = 5.0, 2.5 Hz, 1H), 3.75 (dd, J = 19.1, 7.0 Hz, 1H), 2.50 (ddd, J = 24.2, 18.9, 9.6 Hz, 1H), 2.40 (t, J = 4.8 Hz, 1H), 2.01 – 1.90 (m, 2H), 1.87 – 1.76 (m, 1H), 1.67 (dddd, J = 20.0, 13.2, 6.9, 2.4 Hz, 1H), 1.44 (s, 1H), 1.30 (d, J = 10.2 Hz, 1H), 1.29 – 1.13 (m, 2H).

Development of a kinetic model

We studied the kinetics of the reaction of DCPD with LA to develop a kinetic model to determine the reaction rate and activation energy. The following equation shows the two steps in the esterification of DCPD. The first step includes the hydration of DCPD, and the second step is related to the esterification of the DCPD-OH with LA.



Esterification reactions are known to be second-order reversible reactions.¹⁻³



For the simplicity, equation (2) can be written as following with the restrictions that $C_{A0} = C_{B0}$ and $C_{E0} = C_{W0}$,³

$$-r_A = -\frac{dC_A}{dt} = C_{A0} \frac{dX_A}{dt} = k_2 C_A C_B - k_{-2} C_E C_W = k_2 C_{A0} (1 - X_A)^2 - k_{-2} (C_{A0} X_B)^2 \quad (3)$$

where k_2 and k_{-2} are the apparent forward and reverse rate constants and A, B, E, and W are DCPD-OH, LA, DCPD-LA, and H₂O, respectively. As the esterification between DCPD-OH and LA (second step) is expected to be slower than the first step (hydration) (Fig. 2d,e), we postulated that the concentration of DCPD-OH is similar to the concentration of DCPD. At equilibrium, the equilibrium constant can be expressed by $K = k_2/k_{-2}$, with the fraction of A as $K = (X_{Ae})^2/(1 - X_{Ae})^2$. The above equations can be solved to obtain the values of rate constants, where X_{Ae} corresponds to the fractional conversion of DCPD in equilibrium.³ It is considered that the reverse reaction k_{-2} is relatively small compared to the apparent forward reaction rate constant.¹⁻³ Hence, with the conversion measured in terms of X_{Ae} , this can be indicated as a pseudo second-order reversible reaction which gives the following equation.

$$\ln \left[\frac{X_{Ae} - 2(X_{Ae} - 1)}{X_{Ae} - X_A} \right] = 2k_2 \left(\frac{1}{X_{Ae}} - 1 \right) C_{B0} \times t \quad (4)$$

Then, it can be examined the rate constant with temperature by an Arrhenius' law relationship by plotting $\ln k_2$ versus $1/T$.³ Substituting these values in Arrhenius Eq. (9) gave the activation energy as 16.4 kJ mol⁻¹. In the literature, the activation energy of levulinic acid esterification ranges from 14–51 kJ mol⁻¹, and the sulfated SO₄²⁻/ZrO₂-membrane showed 14.6 kJ mol⁻¹.⁴ The activation energy obtained in this study is comparable with the reported activation energy for the liquid phase esterification.

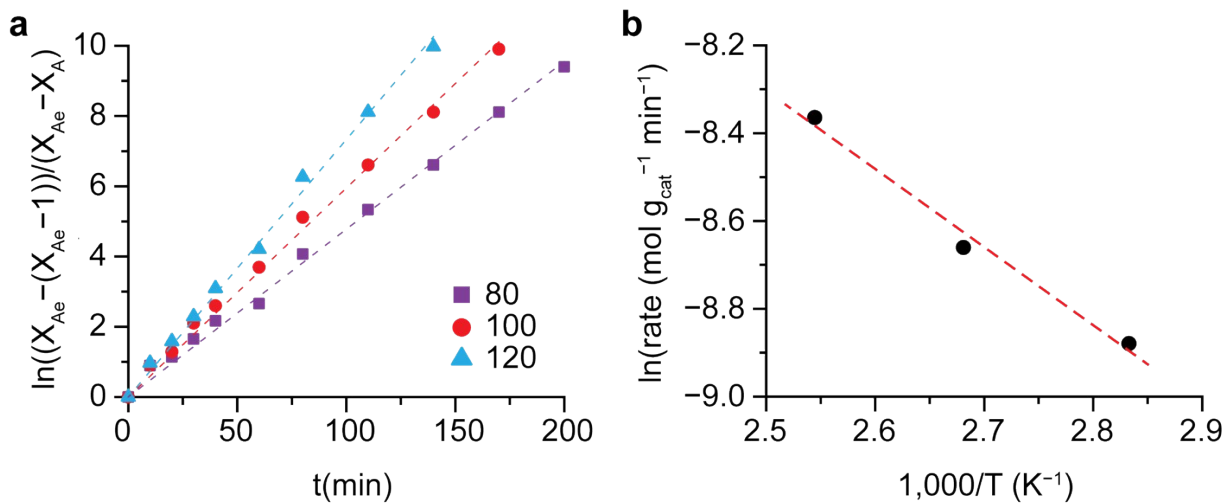


Fig. S3. (a) Plot of kinetic model for DCPD esterification with levulinic acid at different reaction temperatures (80, 100 and 120°C). Reaction conditions: mole ratio (DCPD:LA) = 1:1, Catalyst loading of 20 g-dry resin/L, toluene as solvent. (b) Arrhenius plot of the rate of the DCPD esterification with LA as a function of $1,000/T$.

With the increase in temperature from 80 to 120°C, the rate of DCPD conversion was increased and the complete conversion of DCPD was reached faster at 120°C (Fig. S4a,b). It is important to note that the selectivity to DCPD-LA ester became lower when the temperature increased. For example, after 1 h of reaction at 120°C (Fig. S16), the DCPD-LA yield gradually decreased to 61% after 4 h of reaction, indicating that the DCPD-LA ester was further converted to side products. A side products was analyzed by GC-MS, showing the molecular weights of 266 g mol⁻¹. We postulate this side product as hydroxy-DCPD-LA (OH-DCPD-LA), having hydroxy group on the cyclopentene ring.

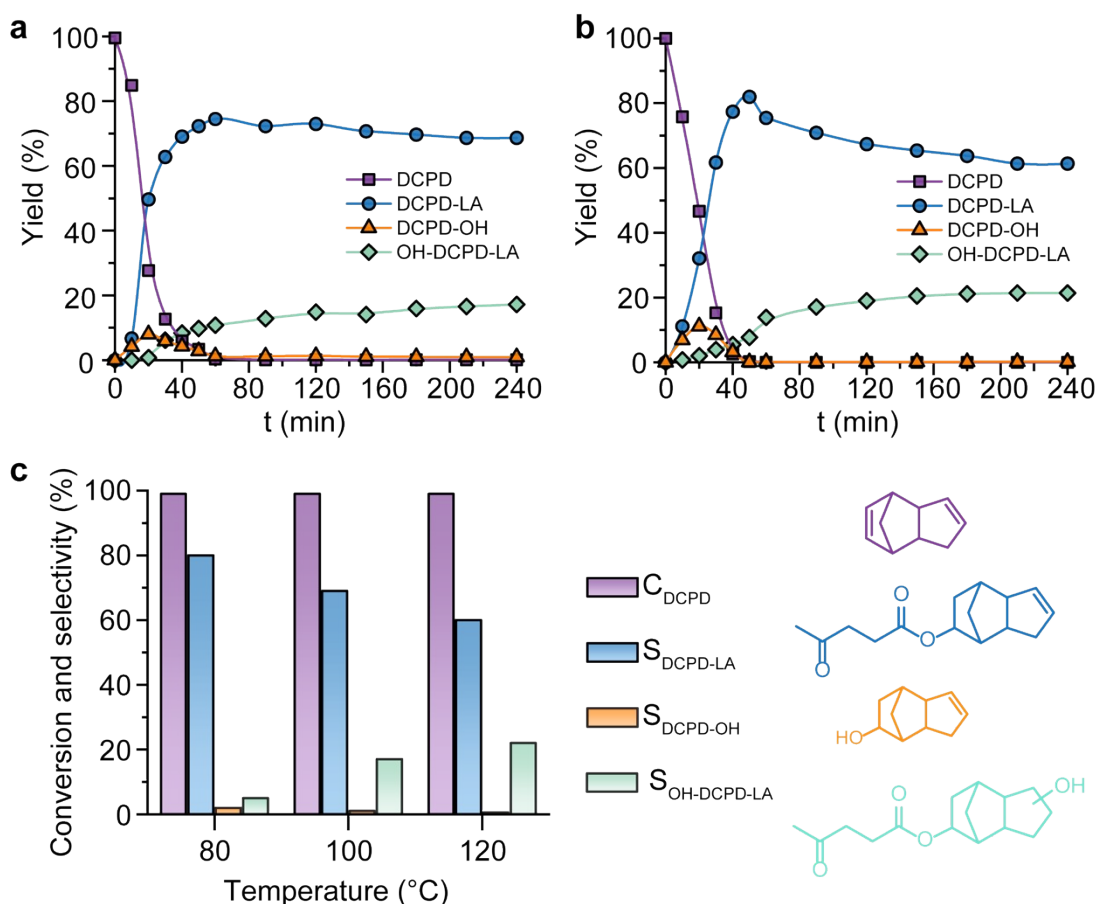


Fig. S4. Esterification results between DCPD with LA at different reaction temperatures. (a) 100°C and (b) 120°C. (c) DCPD conversion and product selectivities (DCPD-LA, DCPD-OH, and OH-DCPD-LA) at the 4 h reaction time at different reaction temperatures.

Analysis of DCPD esters from formic acid (FA), acetic acid (AcA), acrylic acid (AA), butyric acid (BA), and hexanoic acid (HA)

The following figures (Fig. S5–S9) illustrate the GC–MS results of the synthesized esters (DCPD-FA, DCPD-AcA, DCPD-AA, DCPD-BA and DCPD-HA), after separation of the esterification products by column chromatography. The fragmentation patterns of the ester products are related to DCPD and the corresponding carboxylic acid.

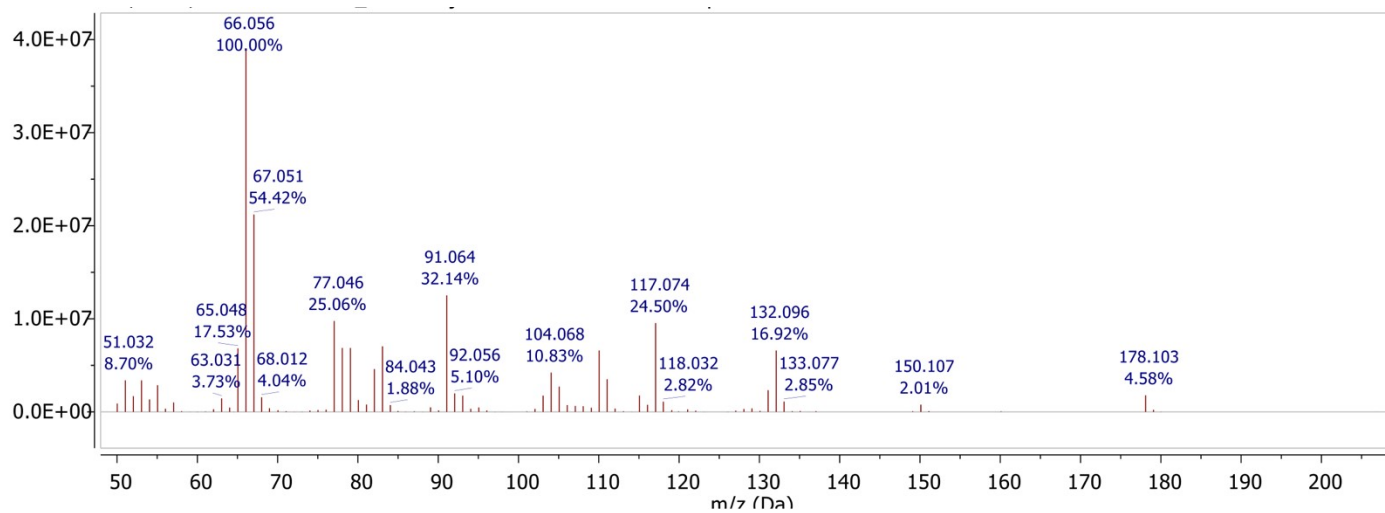


Fig. S5. GC-MS results of DCPD-FA.

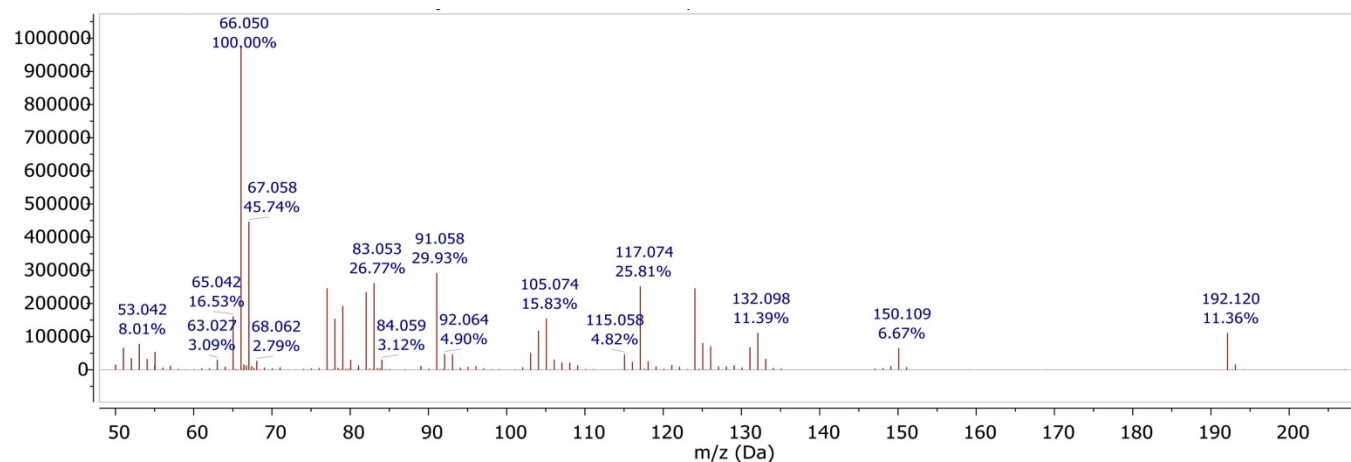


Fig. S6. GC-MS results of DCPD-AcA.

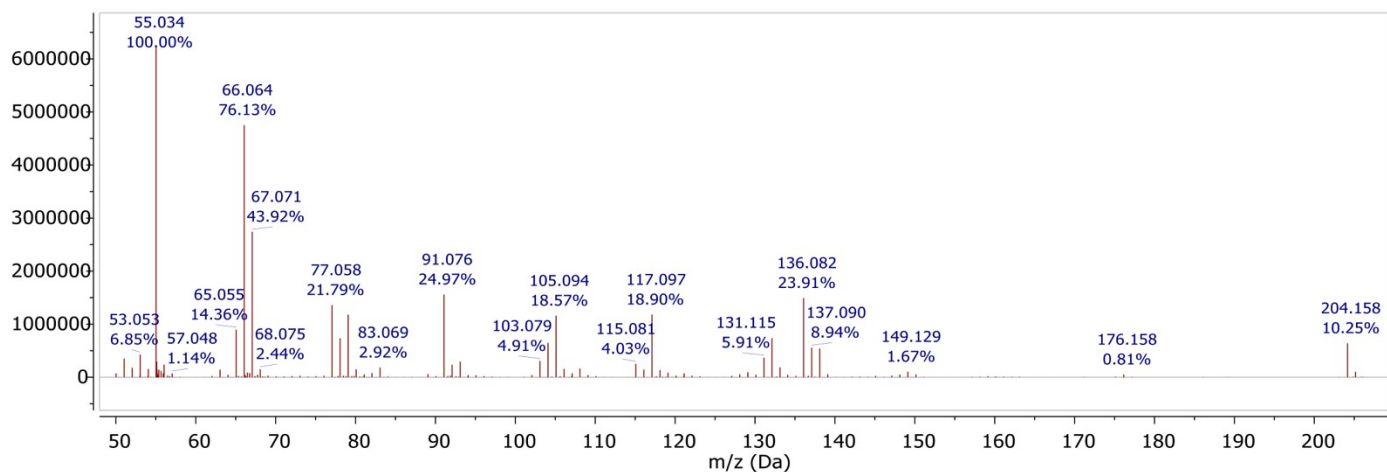


Fig. S7. GC-MS results of DCPD-AA.

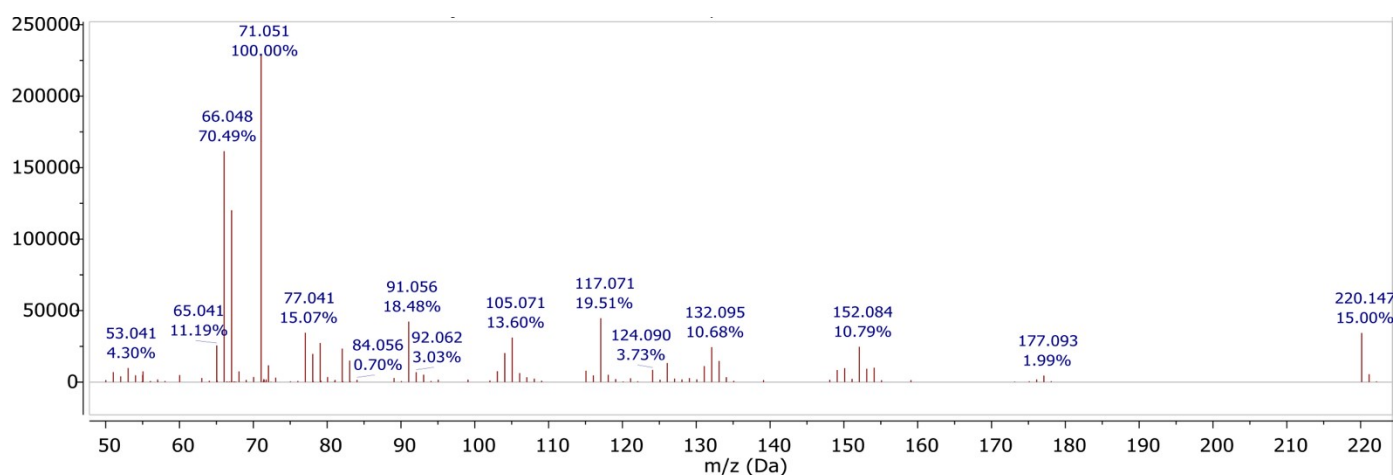


Fig. S8. GC-MS results of DCPD-BA.

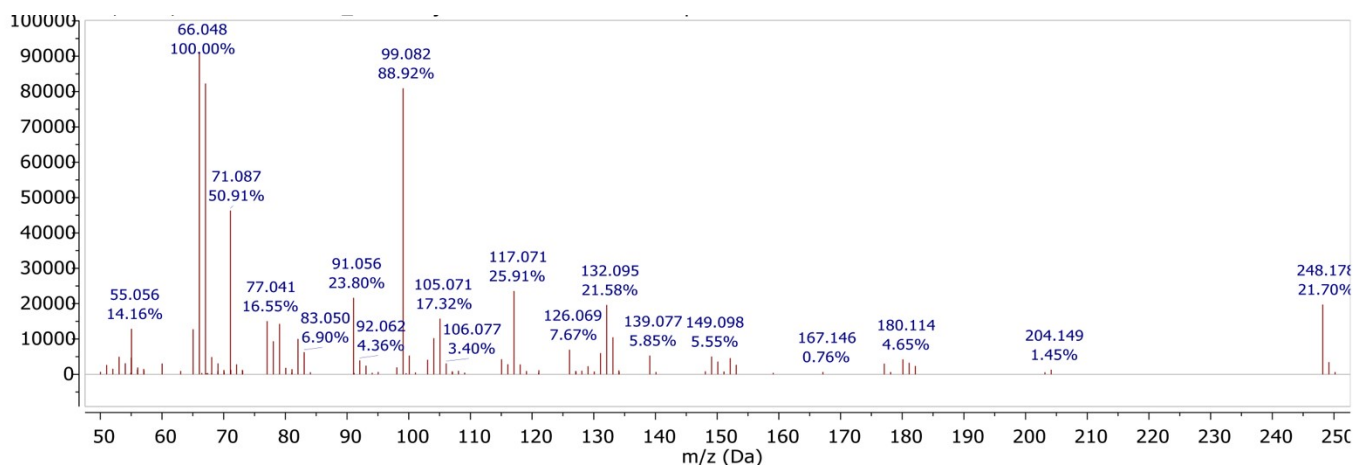


Fig. S9. GC-MS results of DCPD-HA.

In addition, ^1H NMR can also give supplementary information to confirm the structure of the ester products. The following figures (Fig. S10–S14) show the ^1H NMR spectra of the synthesized esters.

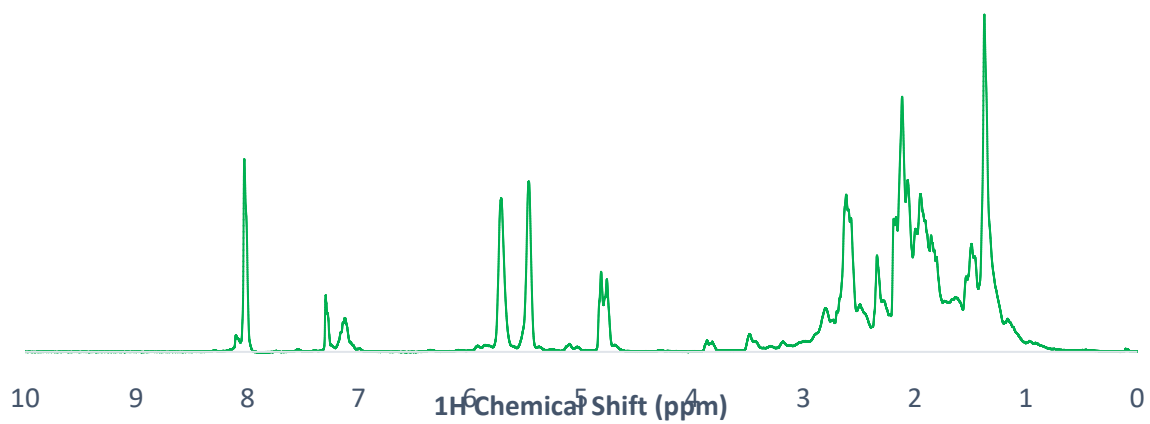


Fig. S10. ¹H NMR spectrum of DCPD-FA.

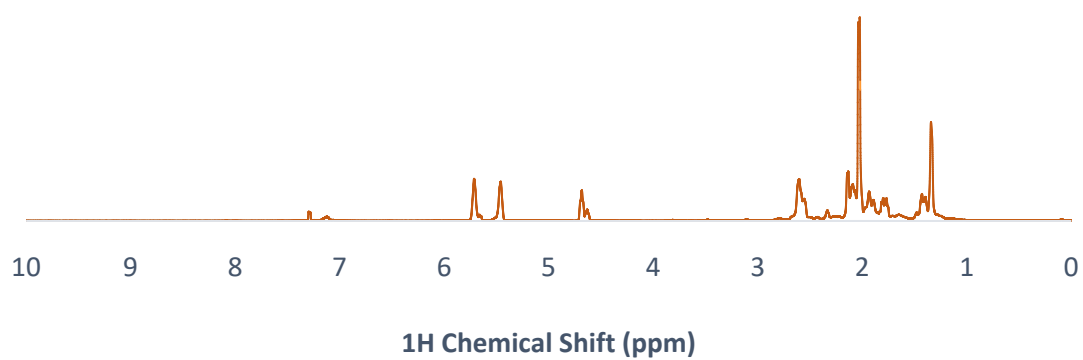


Fig. S11. ¹H NMR spectrum of DCPD-AcA.

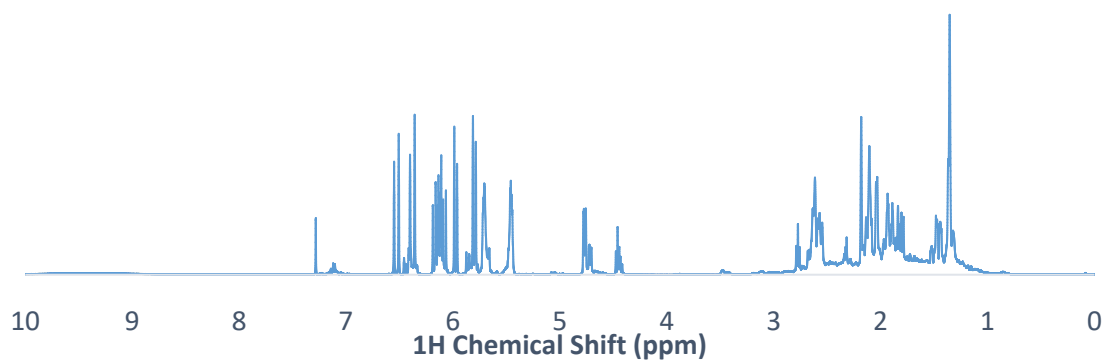


Fig. S12. ¹H NMR spectrum of DCPD-AA.

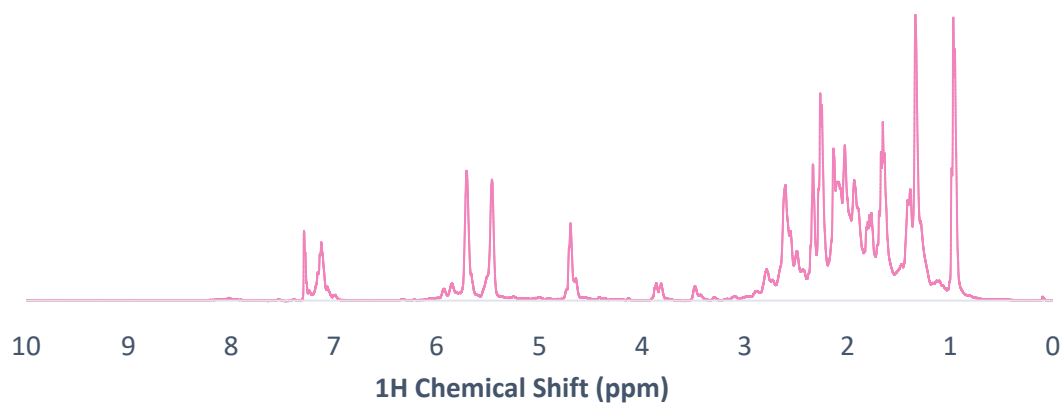


Fig. S13. ^1H NMR Spectrum of DCPD-BA.

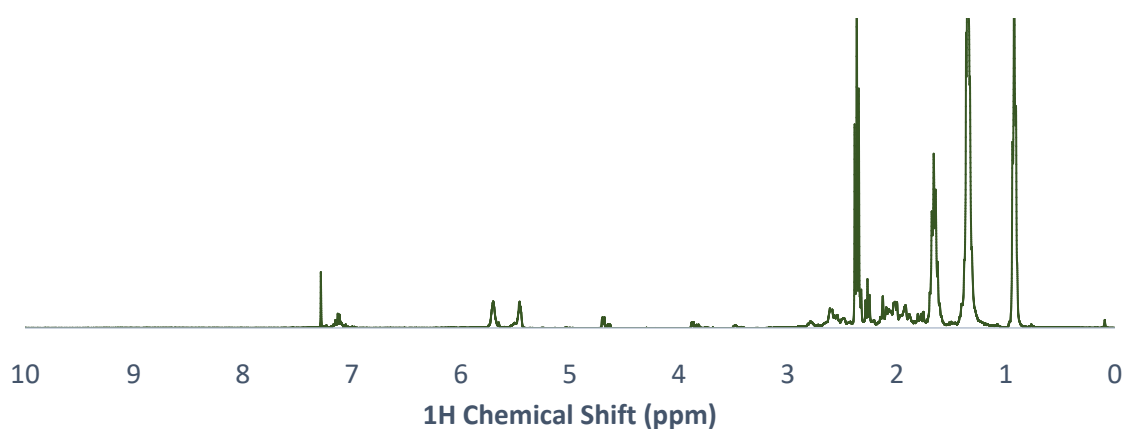


Fig. S14. ^1H NMR Spectrum of DPCD-HA.

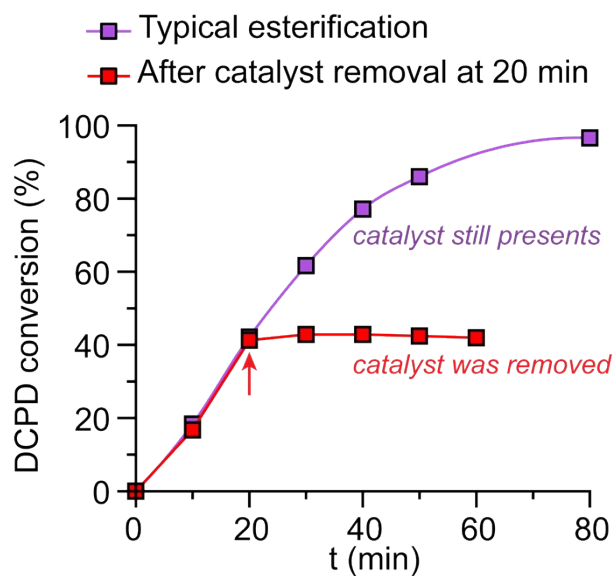


Fig. S15. Leaching test of Amberlyst-15 (hydrogen form) during the esterification of DCPD with LA at 80°C (mole ratio (DCPD:LA) = 1:1, Catalyst loading = 20 g-dry resin/L).

References

1. K. Scott, in *Handbook of Industrial Membranes*, ed. K. Scott, Elsevier Science, Amsterdam, 1995, DOI: <https://doi.org/10.1016/B978-185617233-2/50008-8>, pp. 331-351.
2. J. Caro, in *Comprehensive Membrane Science and Engineering (Second Edition)*, eds. E. Drioli, L. Giorno and E. Fontananova, Elsevier, Oxford, 2017, DOI: <https://doi.org/10.1016/B978-0-12-409547-2.12248-6>, pp. 1-29.
3. M. Mandake, S. Anekar and S. Walke, *American International Journal of Research in Science, Technology, Engineering & Mathematics*, 2013, **3**, 114-121.
4. M. M. Zainol, N. A. S. Amin and M. Asmadi, *Renewable Energy*, 2019, **130**, 547-557.